IEEE Access
Multidisciplinary | Rapid Review | Open Access Journal

Received February 29, 2020, accepted March 8, 2020, date of publication March 11, 2020, date of current version March 20, 2020.

Digital Object Identifier 10.1109/ACCESS.2020.2979991

Combining Chrominance Features and Fast ICA for Noncontact Imaging Photoplethysmography

KEN CAI[1,2], HONGWEI YUE[3], BOHAN LI[4], WEITONG CHEN[5], AND WENHUA HUANG[1,6,7,8]

[1]Guangdong Provincial Key Laboratory of Medical Biomechanics, School of Basic Medical Sciences, Southern Medical University, Guangzhou 510515, China
[2]College of Automation, Zhongkai University of Agriculture and Engineering, Guangzhou 510225, China
[3]Faculty of Intelligent Manufacturing, Wuyi University, Jiangmen 529020, China
[4]College of Computer Science and Technology, Nanjing University of Aeronautics and Astronautics, Nanjing 211106, China
[5]School of Information Technology and Electrical Engineering, The University of Queensland, Brisbane, QLD 4072, Australia
[6]Guangdong Engineering Research Center for Translation of Medical 3D Printing Application, Southern Medical University, Guangzhou 510515, China
[7]Guangdong Innovation Platform for Translation of 3D Printing Application, Southern Medical University, Guangzhou 510515, China
[8]Orthopaedic Center, Affiliated Hospital of Guangdong Medical University, Guangdong Medical University, Zhanjiang 524002, China

Corresponding author: Wenhua Huang (huangwenhua2009@139.com)

This work was supported in part by the National Key R&D Program of China under Grant 2017YFC1103400, the National Natural Science Foundation of China under Grant 21773199 and Grant 31972915, the China Postdoctoral Science Foundation under Grant 2018T110880 and Grant 2017M620375, the Jiangmen Brain-like Computation and Hybrid Intelligence R&D Center ([2018]359, [2019]26), the Science Foundation for Young Teachers of Wuyi University under Grant 2018TD01, the Special Program for National Key Field of Guangdong Province under Grant 2019KQNCX073, the Sanming Project of Medicine in Shenzhen under Grant SZSM201612019, the Science Research Program of Foshan City under Grant 2019012.

ABSTRACT Video-based noncontact detection of heart rate has a wide range of applications in the field of medicine and health. However, this method is susceptible to noise interference, making it difficult to effectively extract blood volume pulse (BVP) signals. To overcome this problem, a new method of noncontact heart rate estimation that can suppress noise interference is proposed in this paper. First, the established data acquisition system conducts video collection, and the captured videos are divided into multiple small regions. Subsequently, the initial signals of BVP are extracted in accordance with the chrominance features extracted through multi-channel data fusion. The BVP signals are separated using the FastICA algorithm. The kurtosis value and signal-to-noise ratios of the power spectrum of the separated signals are analyzed to determine the effective separation component. Results show that this method can extract and process pulse signals, effectively suppressing non-periodic interference. The experiment also proves that the method has good consistency with the measurement of pulse oximeter and has good stability and accuracy in the detection of heart rate of the human body.

INDEX TERMS Chrominance features, kurtosis, photoplethysmography(PPG), data harvesting fusion.

I. INTRODUCTION

Heart rate is an important indicator that reflects the physiological health of the human body and has important applications in the clinical study of cardiovascular disease [1] and physical exercise [2]. Traditional instruments used to measure heart rate include probes and sensors, which can cause discomfort and increase infection risk during long-term use.

In recent years, the development of noncontact heart rate detection and estimation has become a research hotspot in the field of physiological information monitoring to overcome the limitations of traditional instruments. Scholars have proposed a number of methods for noncontact heart rate detection and estimation, including ultrasonic detection, thermodynamic imaging, and photoplethysmography (PPG) [3]–[5]. Recent studies have shown that heart rate can be determined by analyzing skin color changes in video signals. This noncontact and inexpensive method can also be used in certain special scenarios, such as skin damage, neonatal care, and imperceptible monitoring situations [6]–[8]. With the continuous development of noncontact measurement technology, imaging photoplethysmography (PPG)iPPG can provide convenience and comfort and reduce medical costs given that it only requires the processing of body skin color from videos to monitor heart rates automatically by means of data fusion and analysis. Therefore, such research has important practical significance.

The associate editor coordinating the review of this manuscript and approving it for publication was Zhihan Lv.

II. RELATED WORKS

PPG provides the most basic physiological signal of the human body, including hemodynamics [9] and circulation

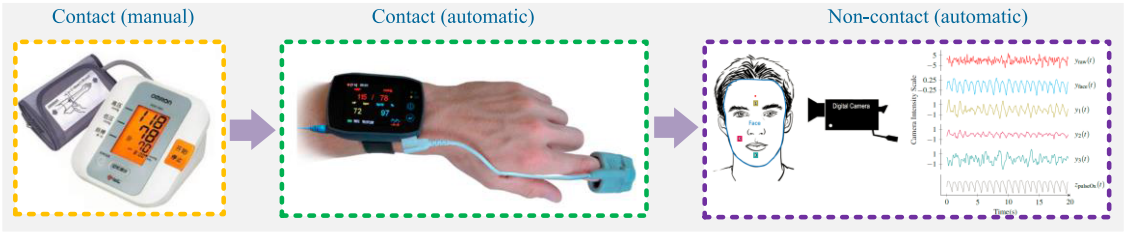

FIGURE 1. Development of heart rate physiological signal detection technology.

information of the autonomic nervous system [10], which is comprehensively displayed in pulse waves, amplitudes, wave speed, and rhythm. These parameters are an important basis for evaluating human physiological state and clinical diagnosis [11] in medicine. The detection technology of physiological signals has developed from contact to noncontact processes, as shown in Figure 1.

In recent years, the noncontact measurement of physiological signals in the human body has been continuously developed. In 2007, Pavlidis used an infrared camera to measure heart rate, respiratory rate, and stress levels. Researchers have demonstrated the effectiveness of using facial thermal imaging systems to calculate physiological signals. Research shows that the conduction cycle, morphological parameters, and rising time can be extracted from PPG signals for physiological evaluation [12]–[14].

At present, obtaining accurate physiological parameters has been the focus of research on noncontact heart rate estimation based on video images. With the development of feature extraction technology [15]–[17], many studies have researched on noncontact heart rate estimation technology using human faces as video objects. In particular, ICA technology has been widely used in heart rate estimation. In 2014, iPPG signals were extracted using a constrained independent component analysis (ICA) method and adaptive filters [18]. Favilla *et al.* used ICA pre-processing to enhance iPPG signals from different regions of the face [19]. Zhang *et al.* proposed a six-channel ICA algorithm to separate more potential sources from smartphone videos [20]. Alghoul *et al.* used ICA algorithms for blind source separation (BSS) to decrease noise interference [21]. However, when the non-skin region of the face produces a large disturbance and the frequency of disturbance is closely related to heart rate (e.g., blinking of the eyes), this method cannot easily filter such disturbance. Using pixel-based rPPG sensors, Wang *et al.* performed ICA to distinguish pulse signals from motion-induced noise using the spatial redundancy of image sensors and estimated the heart rate [22]. And the above studies did not provide a basis to select components after BSS.

In 2016, Wang proposed the spatial subspace rotation (SSR) algorithm to complete pulse extraction by detecting time-domain rotation parameters between the subspaces of the skin color pixel space. This method shows improved anti-interference ability [23]. Notably, in 2016, Wang introduced the plane orthogonal to skin (POS) model, which uses CHROM's information and knowledge of blood volume pulses (BVPs) to define a rough projection region on a skin tone plane and accurately calculate the projection direction on the plane by real-time adjustment [24]. The novelty of POS lies in defining a plane, that is, orthogonal in the color plane of the time-normalized RGB space. This plane is used for pulse extraction. The POS model has better anti-interference capability compared with other models. Invariant features are introduced with respect to the action of a differentiable local group of local transformations [25]. Results show that the energy of the blood volume signal is rearranged in vector space with a more concentrated distribution. Moreover, the recursive probabilistic inference problem in time-varying linear dynamic systems has been addressed to incorporate the invariance into the task of heart rate estimation from face videos under realistic conditions [5].

As reported in the literature, the method of estimating heart rate based on noncontact videos has almost always evolved in accordance with the PPG principle. The relevant medical research on PPG has shown that the temperature of the human body's surrounding environment and the temperature of the epidermal tissue directly affect the perfusion of skin blood flow, which causes great interference on the iPPG signal, decreasing the estimation accuracy of blood oxygen saturation and heart rate. This previous finding also shows that changes in lighting and subjects' slight movements can decrease the accuracy and stability of the heart rate measurement based on the PPG principle. With the development of technology [26]–[28], some scholars have also used deep learning to measure physiological parameters. Since this is not the focus of this article, it will not be described in detail here.

Weak BVP signals can be completely submerged, and their waveforms can be distorted due to noise interference, leading to inaccurate information. These various interference superpositions set strict requirements for filtering non-BVP signals [29]. The signal denoising method has always been the focus of research in the field of signal processing. The anti-interference processing using the BSS method has been applied in many engineering fields. ICA is a signal separation algorithm developed using the BSS problem. Compared with the traditional BSS algorithm, the ICA algorithm is based on high-order statistics of the data for signal processing, and the separated components are not only uncorrelated with each other but are also independent as possible in high-order statistics, thereby reflecting the essential characteristics of the data. The FastICA algorithm is the most common ICA method and

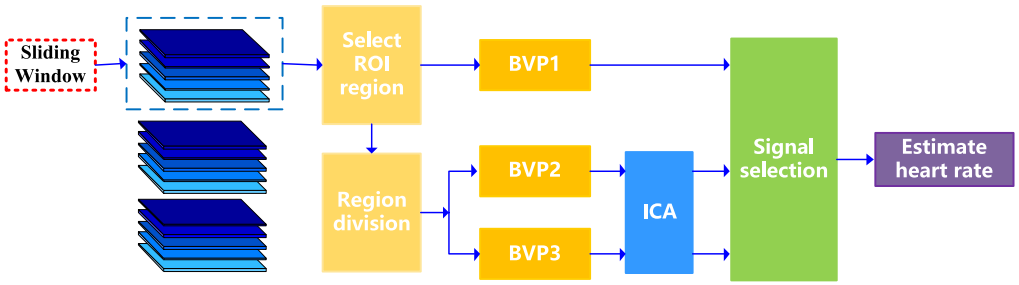

FIGURE 2. Specific process of heart rate estimation.

includes kurtosis-based, maximum likelihood, and maximum negative entropy. The FastICA algorithm based on maximum negative entropy is used in this paper. This method is used to effectively remove the effect of noise. The advantages of this method in denoising have been confirmed by many researchers. However, on the one hand, extracting weak signals from mixed signals using this method alone is difficult under the background of strong noise. On the other hand, many components are obtained using this method. Only a few components are closely related to BVP signals, whereas the rest are irrelevant or interference components. Thus, selecting effective components is necessary to highlight the signal characteristics.

In accordance with previous research, POS and FastICA algorithms are combined in this paper to establish a method of heart rate detection by extracting and denoising BVP signals based on chrominance features. This method removes the noise in BVP signals while retaining useful information. Given that the kurtosis index can quantitatively evaluate the random noise contained in the signal and has the advantages of fast calculation speed, simple algorithm, and strong anti-interference ability, the effective separation component is determined in accordance with the size of the kurtosis value. Results show that this method can adapt to pulse signal analysis and processing and significantly improves the signal-to-noise ratio (SNR) of the pulse wave.

The rest of the paper is organized as follows. The theoretical background is discussed in Part III. In this section, a method for denoising and extracting BVP is provided. The experimental results and evaluation indicators are discussed in detail in Part IV. Part V states the conclusions of this work.

III. METHODOLOGY

The key problem for heart rate estimation based on videos is the accurate estimation of BVP signals from the video images. The heart rate estimation method proposed in this paper considers the effects of incident light, epidermis and subcutaneous reflection, and camera noise; establishes the BVP signal acquisition model; introduces chrominance features and FastICA to eliminate the interference caused by light and movement; and obtains robust heart rate estimation results. The method of estimating heart rate consists of four important steps: (1) detection of the region of interest (ROI), (2) completion of BVP signal extraction, (3) use of FastICA to complete signal denoising, and (4) selection of signal components and estimation of heart rate. Figure 2 shows the specific process of heart rate estimation.

A. EXTRACTION OF CHROMINANCE FEATURES

The iPPG system directly collects the original video containing the pulse wave information, which requires obtaining the pulse wave signal with high SNR. Thus, finding an algorithm with strong anti-interference ability is necessary to complete the extraction of the original pulse signal. At present, the acquisition of one-dimensional iPPG signal is mainly obtained by averaging sensitive regions. However, this method does not achieve efficient separation of the specular reflection component and the pulse component. In this paper, the POS model is used to complete the extraction of chrominance features for the iPPG signal [24].

The POS model uses CHROM's information and knowledge of BVP in defining a rough projection region on the skin color direction plane and in accurately calculating the projection direction on the plane by real-time adjustment to achieve the extraction of chrominance features. This algorithm fuses the data of the three channels, which improves the robustness of the iPPG signal and effectively suppresses the interference of noisy signals. Using the R, G, and B channels, the formula for calculating the chrominance features is as follows:

$$h(t) = S_1(t) + \alpha \cdot S_2(t) \tag{1}$$

where $\alpha = \frac{\sigma(S_1)}{\sigma(S_2)}$, $\sigma(\cdot)$ represents the standard deviation operator. $S_1(t)$ and $S_2(t)$ represent a time-normalized RGB signal combination, $S_1(t) = G(t) - B(t)$ and $S_2(t) = G(t) + B(t) - 2R(t)$, respectively.

The POS method defines the linear combination of specular reflection and pulse components by using skin color features. When the pulse component dominates $h(t)$, $S_1(t)$ and $S_2(t)$ appear in the same phase.The two in-phase signals can increase the resulting signal strength. When the specular reflection dominates $h(t)$, $S_1(t)$ and $S_2(t)$ appear as anti-phases,and α can adjust the specular reflection intensity of one signal to the same level as the other, that is, $\sigma(S_1) = \sigma(\alpha \cdot S_2)$. Then, the two anti-phase signals offset the distortion of specular reflection. However, this method does not enhance heart rate estimation when the interference is

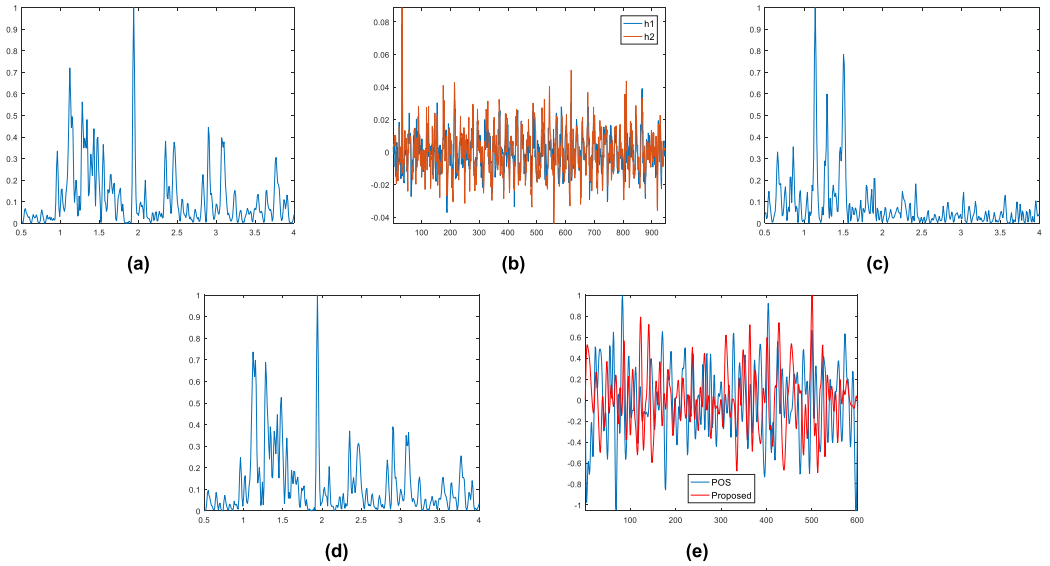

FIGURE 3. Extraction of blood volume pulse. (a) Spectrogram of BVP extracted from the entire region. (b) BVP signal extracted from two sub-regions. (c,d) Spectrogram of independent component signals extracted by FastICA. (e) Extracted time-domain pulse signal.

very severe. The spectrogram in Figure 3(a) shows that the extracted blood volume signal is heavily disturbed by noise. During the test, the subjects are severely disturbed by noise.

B. FASTICA

From the previous description, the POS method defines the linear combination of specular reflection and pulse components by using skin color features. However, if the specular reflection component is highly dominant, obtaining a good signal using the above method alone is difficult. In this paper, the BSS method is used for denoising. ICA is a method for BSS. Using the independence and non-Gaussian nature of the source signal, the method gradually separates several independent useful signals from the unknown mixed signal through a demixing system [30]. FastICA, which is part of ICA, is a fast-finding iteration algorithm that uses fixed-point iterations with simple structure and rapid convergence.

Let the source signal be $S(t) = [S_1(t), S_2(t), \ldots\ldots, S_n(t)]^{\mathrm{T}}$, where $S_i(t)(i = 1, 2, \ldots, n)$ are independent of each other, and at most one obeys the Gaussian distribution. The observed signal is $X(t)$, where $X(t) = B \cdot S(t)$ and B are a mixed matrix with a dimension of $m \times n$. The essence of the FastICA method is to use $X(t)$ to find a demixing matrix W, which maximizes the independence between the components of the output signal $Y(t) = W^{\mathrm{T}}X(t)$.

Studies have shown that non-Gaussianity can be used to characterize the mutual independence of the different components. In components with the same variance, Gaussian components have the greatest entropy. Thus, entropy can be used to measure non-Gaussianity and characterize the independence between components. The modified form of entropy, that is, negative entropy, is generally used.

$$N_g(Y) = H(Y_{Gauss}) - H(Y) \tag{2}$$

In the formula, Y is a random component, Y_{Gauss} is a Gaussian random component and has the same variance as Y, and $H(\cdot)$ is the differential entropy of the component. The expression of the differential entropy of the random variable Y is

$$H(Y) = -\int p_Y(\xi) \lg p_Y(\xi) d\xi \tag{3}$$

where p_Y is the probability density function of Y. Therefore, the mutual independence of the separation results can be expressed by the non-Gaussianity measurement in the separation process. When the measure of non-Gaussianity reaches the maximum, the separation of independent components is completed. The key to the FastICA algorithm is to find a W that maximizes $N_g(Y) = N_g(W^{\mathrm{T}}X)$.

Given that the probability density distribution function needs to be calculated when calculating the differential entropy, which is difficult to achieve in practical applications, we use Equation (4) to approximate the calculation:

$$N_g(Y) = [E(g(Y)) - E(g(Y_{Gauss}))]^2 \tag{4}$$

where $E(\cdot)$ is a mean function and $g(\cdot)$ is a non-linear function. In this paper, $g(Y) = \tanh(Y)$.

If the observation matrix is X, the FastICA algorithm is used to find the demixing matrix W so that $N_g(W^{\mathrm{T}}X)$ has the maximum non-Gaussian property. The approximate Newton iterative formula for the demixing matrix W is

$$\begin{cases} W^* = E(Xg(W^{\mathrm{T}}X)) - E(Xg'(W^{\mathrm{T}}X))W \\ W = W^* / \|W^*\| \end{cases} \tag{5}$$

where $g'(\cdot)$ is the derivative of the non-linear function and W^* is the temporary matrix.

The specific contents of the FastICA algorithm are not covered in detail in this paper. Interested readers can refer

to the relevant literature. In this paper, the ROI is divided into two parts to extract the BVP signal of the two regions, as shown in Figure 3(b). The two BVP signals are separated by ICA to extract the two independent component signals (Figures 3(c)and 3(d)). As shown in Figure 3(c), the corresponding signal has a more obvious pulse signal than the signal in Figure 3(a). Figure 3(e) shows the time-domain diagram corresponding to Figures 3(a) and 3(c) and exhibits that the pulse wave signal obtained by the method in this paper is smoother than that of other methods.

C. KURTOSIS AND SNR OF PULSE WAVE

As a dimensionless parameter, the value of kurtosis can describe the waveform sharpness of the signal and evaluate how much the impact component is contained in the signal [31]. The calculation formulas are as follows:

$$K = \frac{1}{N}\sum_{n=1}^{N} x(n)^4 \Big/ X_{rms}^4 \tag{6}$$

$$X_{rms} = \sqrt{\frac{1}{N}\sum_{n=1}^{N} x(n)^2} \tag{7}$$

where $x(n)$ is the acquired signal, N is the number of sampling points, and X_{rms} is the root mean square value of the signal $x(n)$.

Kurtosis, which is commonly used to measure the non-Gaussian nature of random variables, is highly sensitive to singular values in the data. When a random variable follows the Gaussian distribution, the normalized kurtosis is zero, and the absolute value of kurtosis increases as non-Gaussianity increases. In the field of signal detection and processing, the sample data in the signal time or frequency domain are regarded as a set of random variables, and the pulse characteristics of the signal in the time or frequency domain can be described as kurtosis. Generally, the more pronounced the peaks of a particular frequency, the larger the kurtosis value of the power spectrum [32]. In the FastICA separation results of pulse wave signals, the power spectrum of the BVP component shows a very significant peak in the heartbeat frequency range because of the BVP component's evident quasi-periodicity. In addition, the corresponding kurtosis value is usually large. The other signal component usually does not have a significant spectral peak in the heartbeat frequency range, and the kurtosis value of the corresponding power spectrum is relatively low. According to the frequency-domain pulse characteristics of the BVP signals, the BVP component can be extracted accurately from the two output signals of FastICA by using the kurtosis value. The kurtosis values of the power spectrum in Figures 3(a), (c), and (d) are 10.23, 22.98, and 10.29, respectively.

When the signal has a single-cycle characteristic, the kurtosis value can well distinguish the components of the BSS. However, signals often have multi-cycle characteristics. At this time, the kurtosis value is relatively difficult to distinguish the pulse characteristics of the signal.When the kurtosis

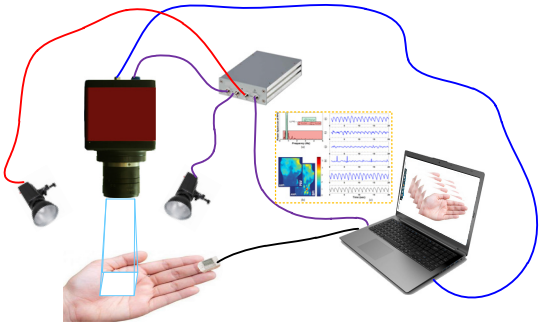

FIGURE 4. Diagrammatic sketch of the experiment for pulse wave extraction.

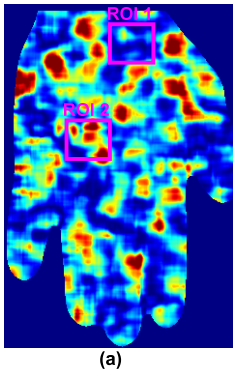

(a)

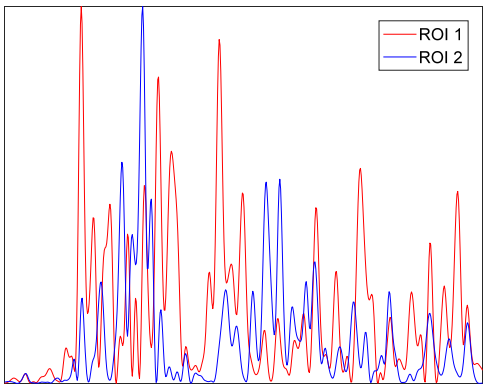

(b)

FIGURE 5. (a) Distribution of the BVP amplitude. (b) Spectrum distribution of ROIs.

values of the power spectrum of the signal is close, using the kurtosis value alone is not a good choice for the signal. In this situation, this paper takes the SNR as another indicator to complete the signal selection. The formula for the SNR is defined as follows:

$$SNR = 10\lg \frac{\sum_{f=0.5}^{4} (U_t(f)\cdot S(f))^2}{\sum_{f=0.5}^{4} (1 - U_t(f))\cdot S(f)^2} \tag{8}$$

In the formula, $S(f)$ represents the spectrum of the extracted pulse signal and $U_t(f)$ is a rectangular window representing the passband of peak in the spectrum

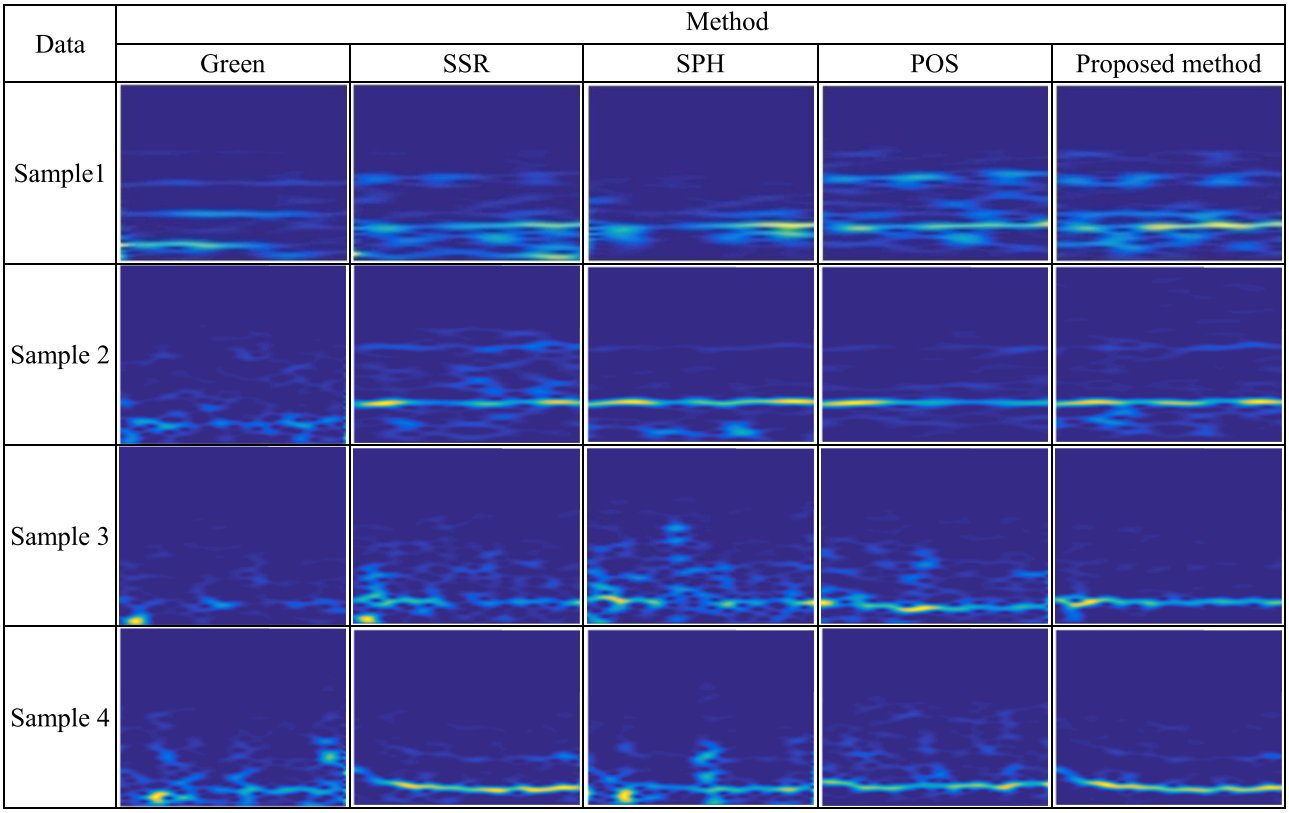

FIGURE 6. Time-frequency analysis of BVP signal of some subjects.

(considered as the true heart rate). The bandwidth used in this paper is 0.4 Hz.

D. FEATURE EXTRACTION METHOD

Although the FastICA method has many advantages in signal extraction, the problem of fuzzy output sorting makes it difficult to automatically acquire BVP. A considerable number of experiments show that the position of the BVP signal is not consistent in the FastICA separation results obtained using different video signals, which makes the BVP automatic acquisition method not easy to implement in practical application. The automatic extraction of BVP signal is necessary to conduct dynamic heart rate estimation. The automatic selection method of BVP based on the kurtosis value of the spectrum is proposed in this paper to solve this problem. The specific implementation steps are as follows:

Step 1. The ROI is divided into two sub-regions, and the pulse signal $h(t)$ of the original region and the pulse signals($h_1(t)$ and $h_2(t)$) of the two sub-regions are extracted, respectively.

Step 2. The FastICA separation is conducted after the preprocessing of $h_1(t)$ and $h_2(t)$ components to obtain signals $Y_1(t)$ and $Y_2(t)$.

Step 3. The kurtosis values and SNRs of the spectrum of $h(t)$, $Y_1(t)$ and $Y_2(t)$ are calculated.

Step 4. If the kurtosis value and SNR of a component's spectrum are both maximum, the component is the BVP signal. Otherwise, $h(t)$ is still used as the BVP signal.

IV. RESULTS AND DISCUSSION

A. EXPERIMENT SCHEME DESIGN

The palm contains several blood vessels, and the blood flow of microvasculature affects the change of the skin's optical characteristics. Based on the PPG principle, the collection of RGB images to obtain this change can acquire signals to calculate physiological parameters such as heart rate, respiratory rate, blood pressure, and heart rate variability. The extraction of heart rate information is only considered in this paper. At the beginning of the experiment, the experimental process is introduced to the volunteers in detail, and a pulse oximeter is clamped on the index finger to measure the heart rate value of the subjects as comparative data. The experimental scenario is shown in Figure 4. The system uses the color CCD as a video acquisition unit, and the collected video data are stored to a computer via the USB interface of the video acquisition card. The video signal is processed by the computer. A total of 60 volunteers are invited to participate in this experiment. During the experiment, the tested persons are divided into two groups, and palm video images are collected under two states (hand shaking and stationary hand), and the acquisition time is approximately 30 s.

B. DISTRIBUTION OF BVP SIGNALS OF THE PALM

The distribution of the intensity of color change caused by the pulse is uneven. In other words, some regions have a large change in color, and some have a small change. Two reasons can explain this uneven distribution: (1) uneven lighting from the light source and (2) the differences in blood volume in different regions caused by the different distribution of blood vessels on the surface of the skin. Under the premise of uniform lighting, the distribution of blood vessels is the main reason for the uneven distribution of color change in the image sequence. By analyzing the distribution of color changes caused by the pulse, the distribution of blood vessels can be roughly analyzed.

This paper uses the distribution of BVP signals to indicate the approximate distribution of microarteries in the palm. Essentially, the distribution of BVP signals reflects the distribution of the intensity of color change in different regions, and these color changes must be caused by the pulse. Figure 5(a) shows the distribution of the BVP amplitude. ROIs 1 and 2 are divided in Figure 5(a), and pulse wave extraction and spectral transformation are performed on these two regions. The result is shown in Figure 5(b). As shown in the figure, the main peak in ROI 2 is more obvious, and the energy is more concentrated. The energy in ROI 1 is relatively dispersed. These results show that when the arterial blood vessels in the local region are relatively small, light changes and respiration are superimposed on each other to form the main signal, forming a strong random and complex interference component.

C. COMPARISON OF DIFFERENT METHODS

The samples collected are used as input samples of algorithms, such as SSR [23], POS [24], SPH [33], and Green [34], to verify the performance of the method described in this paper. In this experiment, the iPPG acquisition system is compared with the finger-clamped pulse oximeter. The following methods are used to complete the BVP signal extraction and time-frequency analysis. Some of the subjects' time-frequency images are shown in Figure 6. In the figure, the horizontal axis is time, the vertical axis is frequency, and the amplitude is represented by the color. During long video-based dynamic heart rate monitoring, the subjects' hand shake may produce unexpected interference components. As shown in Figure 6, the proposed method can take advantage of its interference elimination to obtain a cleaner time-frequency spectrum. Samples 1 and 2 are measured with slight hand shake, and samples 3 and 4 are measured with still hands.

D. OBJECTIVE EVALUATION INDEX

To make the data more intuitive and visual and to show the differences and overall situation of the variables, this paper uses the box diagram for data overview, as shown in Figure 7. In the figure, the middle red line represents the median, and the upper and lower thin lines represent the upper and lower quartiles, respectively. Figure 7(a) shows the measurement results when the hand is stationary, and Figure 7(b) shows the measurement results when the hand is slightly shaken. When the hand remains stationary, the proposed method, SSR, and POS achieved good results; however, the data concentration obtained by the proposed method was higher. In the case where the subject's hand is slightly shaken, the proposed method in this article does not show outliers. The data concentration obtained by the POS method is higher, but outliers appear.

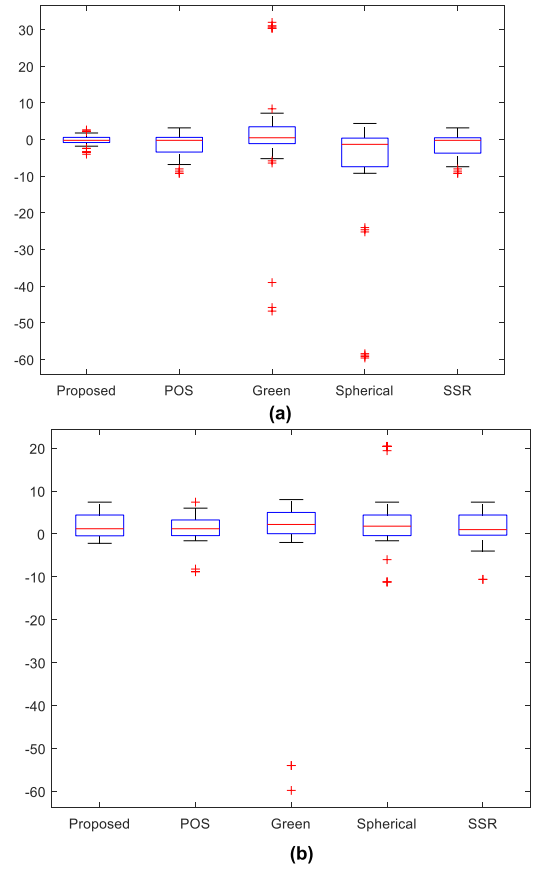

FIGURE 7. Box diagram of heart rate measurement.

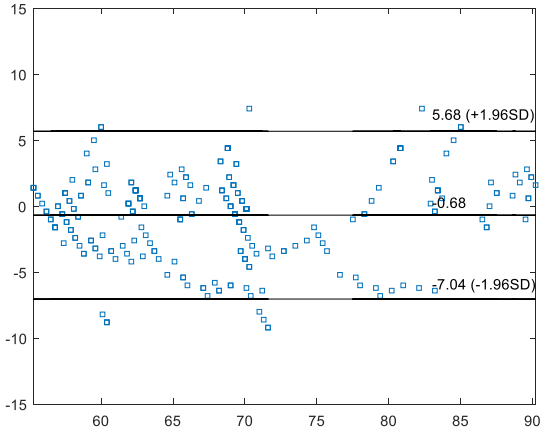

FIGURE 8. Consistency analysis on the proposed method based on Bland–Altman.

E. EXPERIMENTAL VALIDITY ANALYSIS

As this paper explores a new method of noncontact heart rate measurement, the effectiveness of this method is analyzed. The results of video-based heart rate measurements and pulse oximeter measurements are evaluated using the Bland–Altman method. According to statistical analysis, the consistency of the two methods is determined by analyzing the mean and standard deviation of their measurement results. The specific results are shown in Figure 8. The mean, standard deviation, and 95% confidence interval are −0.68, 3.24, and [−7.04 5.68], respectively. The heart rate value obtained by the proposed method shows good consistency with the reference heart rate value, indicating the effectiveness of the video-based heart rate measurement method.

V. CONCLUSION

PPG signal estimation is a crucial step in the extraction of heart rate values from video signals in the common visible spectrum obtained by CCD photoelectric sensor imaging. In our present work, the estimation accuracy is improved by means of data fusion and analysis. Specifically, this paper combined POS and FastICA to extract and denoise pulse signals, realize noncontact heart rate detection in actual indoor conditions, and improve the estimation accuracy. The conclusions drawn in this work are as follows:

1) Combining the kurtosis value with the SNR can better complete the signal selection and heart rate calculation. The BVP component has evident quasi-periodicity, and the corresponding kurtosis value is usually large. The kurtosis index can be used to quantitatively evaluate the random noise contained in the signal, thereby completing the selection of the output signal.

2) The combination of POS and FastICA algorithm can improve the accuracy of heart rate estimation. The linear combination of specular reflection component and pulse component is completed through the POS algorithm, and the initial BVP signal extraction is completed. Then, the blind signal separation technology can be used to effectively filter out the interference signals.

Given that pixel changes in skin images directly reflect changes in iPPG signals, the SNR of the iPPG signals should be improved, which is beneficial for clinical noncontact physiological signal measurement. Notably, the heart rate estimation method cannot accurately estimate the heart rate when the captured video is disturbed by regular interference. Hence, future studies should focus on developing new methods to eliminate any regular interference and further improve the robustness and accuracy of heart rate estimation.

ACKNOWLEDGMENT

(Ken Cai and Hongwei Yue contributed equally to this work.)

REFERENCES

[1] K. S. Parikh, M. A. Greiner, T. Suzuki, and A. D. DeVore, "Resting heart rate and long-term outcomes among the African American population: Insights from the Jackson heart study," *JAMA Cardiol.*, vol. 2, no. 2, pp. 172–180, Feb. 2017.

[2] A. Temko, "Accurate heart rate monitoring during physical exercises using PPG," *IEEE Trans. Biomed. Eng.*, vol. 64, no. 9, pp. 2016–2024, Sep. 2017.

[3] N. Jeger-Madiot, J. Gateau, M. Fink, and R.-K. Ing, "Non-contact and through-clothing measurement of the heart rate using ultrasound vibrocardiography," *Med. Eng. Phys.*, vol. 50, pp. 96–102, Dec. 2017.

[4] C. Bruser, C. H. Antink, T. Wartzek, M. Walter, and S. Leonhardt, "Ambient and unobtrusive cardiorespiratory monitoring techniques," *IEEE Rev. Biomed. Eng.*, vol. 8, pp. 30–43, 2015.

[5] C. S. Pilz, S. Zaunseder, U. Canzler, and J. Krajewski, "Heart rate from face videos under realistic conditions for advanced driver monitoring," *Current Directions Biomed. Eng.*, vol. 3, no. 2, pp. 483–487, Jan. 2017.

[6] M. Villarroel, S. Chaichulee, J. Jorge, S. Davis, G. Green, C. Arteta, A. Zisserman, K. McCormick, P. Watkinson, and L. Tarassenko, "Non-contact physiological monitoring of preterm infants in the neonatal intensive care unit," *NPJ Digit. Med.*, vol. 2, no. 1, pp. 1–18, Dec. 2019.

[7] B.-F. Wu, P.-W. Huang, C.-H. Lin, M.-L. Chung, T.-Y. Tsou, and Y.-L. Wu, "Motion resistant image-photoplethysmography based on spectral peak tracking algorithm," *IEEE Access*, vol. 6, pp. 21621–21634, 2018.

[8] D. Jarchi, P. Charlton, M. Pimentel, A. Casson, L. Tarassenko, and D. A. Clifton, "Estimation of respiratory rate from motion contaminated photoplethysmography signals incorporating accelerometry," *Healthcare Technol. Lett.*, vol. 6, no. 1, pp. 19–26, Feb. 2019.

[9] S. Zaunseder, A. Trumpp, D. Wedekind, and H. Malberg, "Cardiovascular assessment by imaging photoplethysmography—A review," *Biomed. Eng./Biomedizinische Technik*, vol. 63, no. 5, pp. 617–634, Oct. 2018.

[10] A. Hernando, M. D. Pelaez-Coca, M. T. Lozano, M. Aiger, D. Izquierdo, A. Sanchez, M. I. Lopez-Jurado, I. Moura, J. Fidalgo, J. Lazaro, and E. Gil, "Autonomic nervous system measurement in hyperbaric environments using ECG and PPG signals," *IEEE J. Biomed. Health Informat.*, vol. 23, no. 1, pp. 132–142, Jan. 2018.

[11] A. Vallée, A. Cinaud, V. Blachier, H. Lelong, M. E. Safar, and J. Blacher, "Coronary heart disease diagnosis by artificial neural networks including aortic pulse wave velocity index and clinical parameters," *J. Hypertension*, vol. 37, no. 8, pp. 1682–1688, Aug. 2019.

[12] A. A. Kamshilin and N. B. Margaryants, "Origin of photoplethysmographic waveform at green light," *Phys. Procedia*, vol. 86, pp. 72–80, Jan. 2017.

[13] I. Pavlidis, J. Dowdall, and N. Sun, "Interacting with human physiology," *Comput. Vis. Image Understand.*, vol. 108, nos. 1–2, pp. 150–170, Oct./Nov. 2007.

[14] S. Bhat, M. Adam, Y. Hagiwara, and E. Y. K. Ng, "The biophysical parameter measurements from PPG signal," *J. Mech. Med. Biol.*, vol. 17, no. 7, Nov. 2017, Art. no. 1740005.

[15] H. Tang, B. Xiao, W. Li, and G. Wang, "Pixel convolutional neural network for multi-focus image fusion," *Inf. Sci.*, vols. 433–434, pp. 125–141, Apr. 2018.

[16] B. Xiao, K. Wang, X. Bi, W. Li, and J. Han, "2D-LBP: An enhanced local binary feature for texture image classification," *IEEE Trans. Circuits Syst. Video Technol.*, vol. 29, no. 9, pp. 2796–2808, Sep. 2019.

[17] M. R. Faraji and X. Qi, "Face recognition under varying illuminations using logarithmic fractal dimension-based complete eight local directional patterns," *Neurocomputing*, vol. 199, pp. 16–30, Jul. 2016.

[18] F. Peng, Z. Zhang, X. Gou, H. Liu, and W. Wang, "Motion artifact removal from photoplethysmographic signals by combining temporally constrained independent component analysis and adaptive filter," *Biomed. Eng. OnLine*, vol. 13, no. 1, p. 50, Jul. 2014.

[19] R. Favilla, V. C. Zuccala, and G. Coppini, "Heart rate and heart rate variability from single-channel video and ICA integration of multiple signals," *IEEE J. Biomed. Health Informat.*, vol. 23, no. 6, pp. 2398–2408, Nov. 2019.

[20] C. Zhang, X. Wu, L. Zhang, X. He, and Z. Lv, "Simultaneous detection of blink and heart rate using multi-channel ICA from smart phone videos," *Biomed. Signal Process. Control*, vol. 33, pp. 189–200, Mar. 2017.

[21] K. Alghoul, S. Alharthi, H. Al Osman, and A. El Saddik, "Heart rate variability extraction from videos signals: ICA vs. EVM comparison," *IEEE Access*, vol. 5, pp. 4711–4719, 2017.

[22] W. Wang, S. Stuijk, and G. de Haan, "Exploiting spatial redundancy of image sensor for motion robust rPPG," *IEEE Trans. Biomed. Eng.*, vol. 62, no. 2, pp. 415–425, Feb. 2015.

[23] W. Wang, S. Stuijk, and G. de Haan, "A novel algorithm for remote photoplethysmography: Spatial subspace rotation," *IEEE Trans. Biomed. Eng.*, vol. 63, no. 9, pp. 1974–1984, Sep. 2016.

[24] W. Wang, A. C. den Brinker, S. Stuijk, and G. de Haan, "Algorithmic principles of remote PPG," *IEEE Trans. Biomed. Eng.*, vol. 64, no. 7, pp. 1479–1491, Jul. 2017.
[25] C. S. Pilz, S. Zaunseder, J. Krajewski, and V. Blazek, "Local group invariance for heart rate estimation from face videos in the wild," in *Proc. IEEE/CVF Conf. Comput. Vis. Pattern Recognit. Workshops (CVPRW)*, Salt Lake City, Utah, USA, Jun. 2018, pp. 1254–1262.
[26] Z. Huang, X. Xu, J. Ni, H. Zhu, and C. Wang, "Multimodal representation learning for recommendation in Internet of Things," *IEEE Internet Things J.*, vol. 6, no. 6, pp. 10675–10685, Dec. 2019.
[27] B. Wu, T. Cheng, T. L. Yip, and Y. Wang, "Fuzzy logic based dynamic decision-making system for intelligent navigation strategy within inland traffic separation schemes," *Ocean Eng.*, vol. 197, Feb. 2020, Art. no. 106909.
[28] Z. Huang, X. Xu, H. Zhu, and M. Zhou, "An efficient group recommendation model with multiattention-based neural networks," *IEEE Trans. Neural Netw. Learn. Syst.*, to be published, doi: 10.1109/TNNLS.2019.2955567.
[29] M. Khan, C. G. Pretty, A. C. Amies, R. Elliott, Y. S. Chiew, G. M. Shaw, and J. G. Chase, "Analysing the effects of cold, normal, and warm digits on transmittance pulse oximetry," *Biomed. Signal Process. Control*, vol. 26, pp. 34–41, Apr. 2016.
[30] R. Ge, Y. Wang, J. Zhang, L. Yao, H. Zhang, and Z. Long, "Improved FastICA algorithm in fMRI data analysis using the sparsity property of the sources," *J. Neurosci. Methods*, vol. 263, pp. 103–114, Apr. 2016.
[31] T. A. Hearn and L. Reichel, "Image denoising via residual kurtosis minimization," *Numer. Math., Theory, Methods Appl.*, vol. 8, no. 3, pp. 406–424, Aug. 2015.
[32] J. Antoni, "The spectral kurtosis: A useful tool for characterising non-stationary signals," *Mech. Syst. Signal Process.*, vol. 20, no. 2, pp. 282–307, Feb. 2006.
[33] C. Pilz, "On the vector space in photoplethysmography imaging," in *Proc. IEEE/CVF Int. Conf. Comput. Vis. Workshop (ICCVW)*, Seoul, South Korea, Oct. 2019, pp. 1–9.
[34] W. Verkruysse, L. O. Svaasand, and J. S. Nelson, "Remote plethysmographic imaging using ambient light," *Opt. Express*, vol. 16, no. 26, pp. 21434–21445, Dec. 2008.

KEN CAI received the Ph.D. degree in biomedical engineering from the South China University of Technology, China, in 2011. He is currently a Postdoctoral Research Fellow with the School of Basic Medical Sciences, Southern Medical University, China. He is also an Associate Professor with the College of Automation, Zhongkai University of Agriculture and Engineering, China. His current main research interests include medical data analytic, deep learning, pattern recognition, decision making, and biomedical instrument.

HONGWEI YUE received the Ph.D. degree in control theory and control engineering from the Guangdong University of Technology, China, in 2013. He is currently an Associate Professor with the Faculty of Intelligent Manufacturing, Wuyi University, China. His research interests include image processing, biomedical instrument, and information security.

BOHAN LI received the Ph.D. degree in computer application from the Harbin University of Science and Technology, Harbin, in 2009. He is currently an Associate Professor with the College of Computer Science and Technology, Nanjing University of Aeronautics and Astronautics (NUAA), Nanjing. His current research interests include spatio-temporal database, blockchain, sentiment analysis, and so on. He is a member of CCF and ACM.

WEITONG CHEN received the Ph.D. degree in computer science from The University of Queensland, Australia, in 2020. He is currently a Postdoctoral Research Fellow with The University of Queensland, Australia. His current main research interests include medical data analytic, deep learning, data mining, pattern recognition, and social computing.

WENHUA HUANG received the Ph.D. degree in human anatomy from Southern Medical University (First Military Medical University), Guangzhou, China, in 2001. He is currently the Chairman with the School of Basic Medical Science, Southern Medical University, China. His current research interests include the 3D printing technology and computed aided diagnosis.